IEICE TRANS. FUNDAMENTALS, VOL.E83–A, NO.6 JUNE 2000

PAPER *Special Section of Papers Selected from ITC-CSCC'99*

A New Extended Frequency Transformation for Complex Analog Filter Design

Cosy MUTO[†], ***Regular Member***

SUMMARY In this paper, a new frequency transformation for complex analog filter design which is suitable for integration is discussed. Arbitrary specified passband and stopband edges are easily transformed into those of the normalized LPF by solving simultaneous equations with four unknowns. Different from previous methods, the proposed transformation provides better performance in active realization of complex filters.

key words: *complex analog filter design, image rejection filters, frequency transformation, imaginary resistance, complex leapfrog*

1. Introduction

Complex signal processing [1]–[5] is considered useful as a method of high-performance signal processing, especially in the field of communication systems such as orthogonal modulation/demodulation, image rejection filters [6], etc.

There are three kinds of method for designing complex transfer function in analog domain, that is the Lang-Brackett method, frequency shifting and the extended frequency transformation:

The Lang-Brackett method [1] uses a very narrow bandwidth real coefficient BPF as the reference filter. The destination complex filter is obtained by removing unnecessary poles and zeros and shifting its frequency response. There are no design guidelines which provide the prototype BPF, so that it seems to be a so-called "*cut & try*" method.

Frequency shifting [3] simply shifts the frequency response of the prototype filter. Since poles and zeros of a real coefficient filter are located on complex conjugate positions each other, the resultant filter response is always symmetrical with respect to the shifting frequency.

The extended frequency transformation (EFT) [4] can be used in both analog and digital complex filter design. It is based on the frequency transformation from the normalized LPF, which is widely used in conventional filter design. By shifting coordinate axes of a non-linear mapping function, passband and stopband edges of a real reference filter are mapped onto arbitrary specified frequencies. In analog filter design, the Extended LP-HP Transformation (ELHT) is proposed by the author [4]. It provides lowest filter order for given passband and stopband edges, however, its active realization using complex resonators [3] has a controllability problem in applications such as automatic tuning filters [7], [8]. This drawback comes from transformation function itself.

In this paper, we discuss a new frequency transformation for complex analog filter design. At first, we observe an overview of the extended frequency transformation and the ELHT. In Sect. 3, "*lowpass to lowpass*" basis transformation, the Bilinear LP-LP Transformation (BLLT), is proposed. Formulation, parameter decision and reactance transformation are explained there. In Sect. 4, active realization of the passive complex filter designed by BLLT is discussed. A general configuration and an OTA-C realization of the immittance branch simulation using the complex resonators are proposed. Sensitivities of BLLT parameters due to active element deviations and compensation for resonator loss are given. The proposed method does not have the disadvantage which occurs in ELHT. A demonstration of the proposed method is shown in Sect. 5, where a design example illustrates the validity of the proposed method.

2. The Extended Frequency Transformation

2.1 Fundamental Concept

The extended frequency transformation is defined as

$$\omega = f(x : \omega_C, \omega_S, x_S), \tag{1}$$

where $f(x)$ is a transformation function from normalized LPF. Parameters ω and x are frequency variables of destination and reference filters, respectively. $\omega_C > 0$ is the scaling factor, ω_S and x_S are shifting parameters of the coordinate axes of the frequency transformation, respectively.

It is frequently convenient to express Eq. (1) in its inverse form:

$$x = g(\omega : \omega_C, \omega_S, x_S). \tag{2}$$

In this representation, frequencies of the destination complex filter are mapped onto those of normalized LPF. By solving simultaneous equations with respect to appropriate frequencies such as passband and stopband edges, we can determine all the parameters shown above.

Manuscript received September 25, 1999.
Manuscript revised December 27, 1999.

[†]The author is with the Department of Telecommunications, Takuma National College of Technology, Kagawa-ken, 769-1192 Japan.

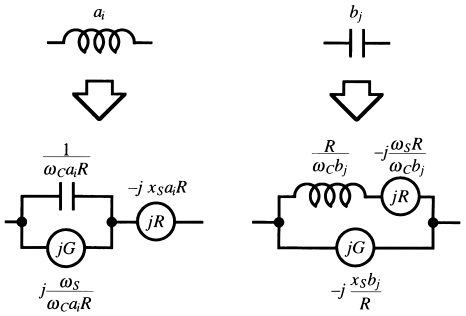

Fig. 1 ELHT reactance transformation.

2.2 The Extended LP-HP Transformation

The Extended LP-HP Transformation (ELHT) [4] is defined by the author in the form of Eq. (2):

$$x = -\frac{\omega_C}{\omega - \omega_S} - x_S. \tag{3}$$

By applying Eq. (3) to passband and stopband edge frequencies of the destination complex filter, we can determine all the parameters and the normalized LPF. Circuit elements of the normalized LPF are transformed as shown in Fig. 1, where jR and jG are imaginary resistance [9], [10] and imaginary conductance, respectively. R denotes terminating resistance.

Branch immittances of an ELHT filter† are given by

$$\left.\begin{aligned} Y_i(s) &= \frac{1}{\dfrac{1}{sC_i + jG_i} + jR_i} \\ C_i &= \frac{1}{\omega_C a_i R} \\ jG_i &= -j\frac{\omega_S}{\omega_C a_i R} \\ jR_i &= -jx_S a_i R \end{aligned}\right\} \tag{4}$$

and

$$\left.\begin{aligned} Z_j(s) &= \frac{1}{\dfrac{1}{sL_j + jR_j} + jG_j} \\ L_j &= \frac{R}{\omega_C b_j} \\ jR_j &= -j\frac{\omega_S R}{\omega_C b_j} \\ jG_j &= -jx_S\frac{b_j}{R}, \end{aligned}\right\} \tag{5}$$

respectively. These are bilinear functions with respect to complex frequency variable s.

3. The Proposed Method: The Bilinear LP-LP Transformation

3.1 Formulation

Consider a following transformation:

$$x = \frac{\omega + c}{a\omega + b}. \tag{6}$$

If the passband and stopband edge frequencies of a complex filter are mapped onto them of the normalized LPF and it provides realizable passive filter structure, we can use the above transformation as another EFT method in analog domain. However, realizability of a passive complex filter using inductors, capacitors, resistors and imaginary resistors should be considered.

Since the equation has slight different form from Eq. (2), we discuss its physical meaning and reactance transformation from the normalized LPF. By rewriting Eq. (6), we have

$$x = -\frac{1}{-\dfrac{\omega_C}{\omega - \omega_S} - x_S} \tag{7}$$

where

$$\left\{\begin{aligned} \omega_C &= b - ac \quad (>0) \\ \omega_S &= -c \\ x_S &= -a. \end{aligned}\right. \tag{8}$$

The denominator of the right hand side of Eq. (7) is the function of ELHT which described in the previous section. This means that the normalized LPF is transformed into the normalized HPF, which is subsequently transformed into complex filter. Therefore, Eq. (7) is interpreted as a special case of the ELHT that the destination complex filter is converted into the normalized HPF.

Since the transformation described in Eq. (6) or Eq. (7) has bilinear form on ω and becomes conventional LP to LP transformation if $\omega_S = x_S = 0$, we designate it "the Bilinear LP-LP Transformation (BLLT)." The BLLT also includes the frequency shifting method [3] if $x_S = 0$. In this point of view, the BLLT is said to be more general design method for complex filters than the ELHT. The concept of the BLLT is illustrated in Fig. 2.

3.2 Parameter Decision, Transfer Function and Stability

The above parameters and the stopband edge of the normalized LPF are given by solving the following simultaneous equations:

†Hereafter, we use this kind of simple expression instead of "complex filter designed by ELHT" throughout this paper.

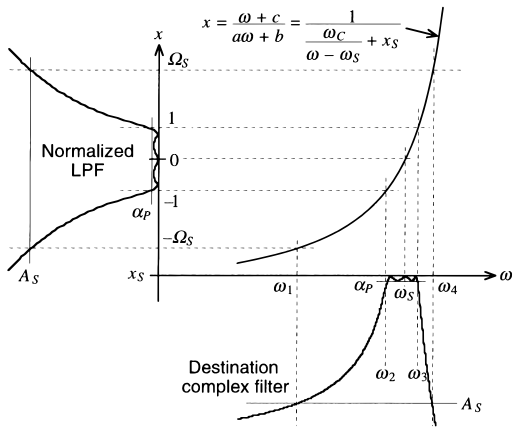

Fig. 2 The bilinear LP-LP transformation.

$$\begin{cases} \Omega_S &= \dfrac{1}{\dfrac{\omega_C}{\omega_4-\omega_S}+x_S} \\ 1 &= \dfrac{1}{\dfrac{\omega_C}{\omega_3-\omega_S}+x_S} \\ -1 &= \dfrac{1}{\dfrac{\omega_C}{\omega_2-\omega_S}+x_S} \\ -\Omega_S &= \dfrac{1}{\dfrac{\omega_C}{\omega_1-\omega_S}+x_S} \end{cases} \tag{9}$$

where Ω_S is the stopband edge of the normalized LPF. There exists two solution sets for Eq. (9), however, one set contains positive ω_C and the other contains negative one. Because $\omega_C > 0$ by definition, selecting the set containing positive ω_C leads correct solution.

The transfer function of the destination complex filter is obtained by the following replacement:

$$p \to \frac{1}{\dfrac{\omega_C}{s-j\omega_S} - jx_S} \tag{10}$$

where p and s are complex frequency variables of the normalized LPF and the destination complex filter, respectively. Any stable pole $p_i = u_i + jv_i$ $(u_i < 0)$ of the normalized LPF is mapped onto

$$p_i' = \frac{u_i}{(1-x_Sv_i)^2+(x_Su_i)^2}\omega_C + j\left\{\frac{v_i - x_S({u_i}^2+{v_i}^2)}{(1-x_Sv_i)^2+(x_Su_i)^2}\omega_C + \omega_S\right\} \tag{11}$$

by the BLLT. Since $u_i < 0$ and $\omega_C > 0$, mapped pole p_i' locates on left-half side of the s-plane. Therefore, the complex filter designed by BLLT is always stable.

3.3 Reactance Transformation

Element values of the passive complex filter designed by BLLT are easily obtained. Inductances and capacitances of the normalized LPF, say, a_i and b_j, are converted into complex one-ports as shown in Fig. 3. Immittances of these arms are given by

$$\left.\begin{aligned} Y_i(s) &= \frac{1}{sL_i+jR_i} + jG_i \\ L_i &= \frac{a_iR}{\omega_C} \\ jR_i &= -j\frac{\omega_Sa_iR}{\omega_C} \\ jG_i &= -j\frac{x_s}{a_iR} \end{aligned}\right\} \tag{12}$$

and

$$\left.\begin{aligned} Z_j(s) &= \frac{1}{sC_j+jG_j} + jR_j \\ C_j &= \frac{b_j}{\omega_CR} \\ jG_j &= -j\frac{\omega_Sb_j}{\omega_CR} \\ jR_j &= -j\frac{x_sR}{b_j}, \end{aligned}\right\} \tag{13}$$

respectively, where R is the termination resistor of the destination complex filter.

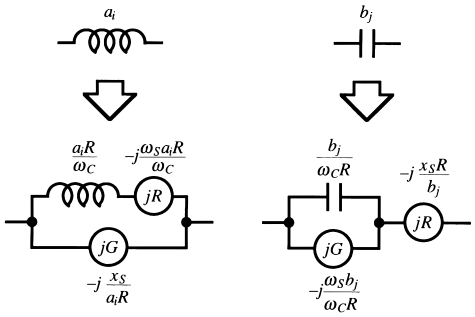

Fig. 3 BLLT reactance transformation.

4. Active Realization of BLLT Filter

4.1 Complex Leapfrog

Low sensitivity property of terminated passive filter [11]–[13] inherits to complex filter case [14]. For this reason, passive filter simulations such as complex leapfrog [5] or imaginary resistance simulation are better than cascading first order complex transfer function blocks. However, imaginary resistance simulation using gyrators or negative impedance converters is sensitive to component deviations and has less dynamic range. Therefore, complex leapfrog provides the best synthesis method among them.

The concept of complex leapfrog is similar to real filter case. In Fig. 4, currents of series admittances and voltages across shunt impedances are given by

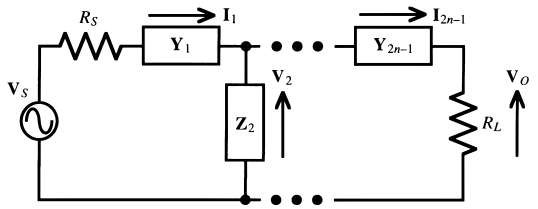

Fig. 4 Concept of the complex leapfrog.

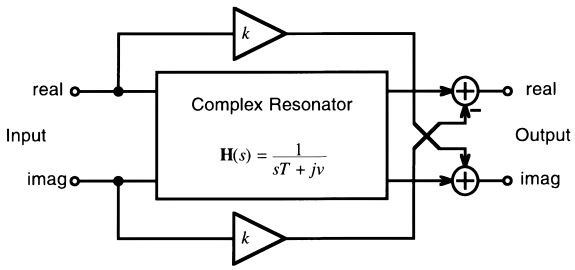

Fig. 5 Conceptual diagram of the bilinear complex resonator.

$$\left.\begin{array}{ll} \mathbf{I}_1 & = Y_1(\mathbf{V}_S - \mathbf{I}_1 R_S - \mathbf{V}_2) \\ \mathbf{V}_2 & = Z_2(\mathbf{I}_1 - \mathbf{I}_3) \\ & \vdots \\ \mathbf{I}_{2n-1} & = Y_{2n-1}(\mathbf{V}_{2n-2} - \mathbf{V}_{2n}) \\ \mathbf{V}_O & = R_L \mathbf{I}_{2n-1}, \end{array}\right\} \tag{14}$$

where $\mathbf{V}_i = V_{ir} + jV_{ii}$ and $\mathbf{I}_j = I_{jr} + jI_{ji}$ are the complex voltages and currents, respectively. The immittances in the above equations are given by Eqs. (12) and (13).

The passive complex filter is then active simulated by using functional blocks which transfer functions are given by

$$\mathbf{T}(s) = \frac{1}{sT + jv} + jk. \tag{15}$$

Since the entire transfer function has a bilinear form on complex frequency variable s, we designate the circuit the bilinear complex resonator.

4.2 An OTA-C Realization of The Bilinear Complex Resonator

The first term of the right hand side in Eq. (15) is the first order complex transfer function. Therefore, transfer functions which simulate immittances expressed by Eqs. (12) and (13) can be active realized by taking weighted sum of the output of the complex resonator [3], [15] and its input signal. Figure 5 shows schematic diagram of the bilinear complex resonator realizing the immittances mentioned in Sect. 3.

An OTA-C realization of the voltage mode bilinear complex resonator is shown in Fig. 6. The transfer function of this resonator is given by

$$\mathbf{H}_C(s) = \frac{g_1}{sC + (g_p - g_c) + jg_2} \frac{g_3}{g_L} + j\frac{g_4}{g_L} \tag{16}$$

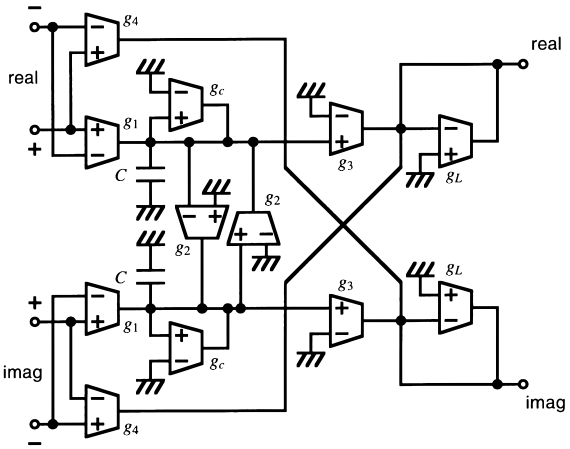

Fig. 6 An OTA-C realization of the bilinear complex resonator.

where g_p is the sum of input conductances of OTA g_2 and g_3. The transconductance g_c is for compensation of resonator loss due to g_p. Element values of the resonator are given by

$$\left.\begin{array}{ll} g_1 = g_3 & = \sqrt{\dfrac{\omega_C C}{k}} \\ g_2 & = -\omega_S C \\ g_4 & = -\dfrac{x_S}{k} \\ g_L & = \dfrac{a_i R}{k} \quad \text{or} \quad \dfrac{b_j}{kR} \\ g_c & = g_p, \end{array}\right\} \tag{17}$$

where k and C are appropriate scaling coefficient, resonator capacitance, and, a_i and b_j are inductance and capacitance of the normalized LPF, respectively. If negative value of transconductance is obtained, both positive and negative input of the corresponding OTA should be interchanged.

4.3 Sensitivity Analysis

In integrated active circuits, relative accuracy between two passive elements is much smaller than their absolute accuracies. In the following analysis, we assume that same valued elements are well matched each other so that device mismatch is not the subject under consideration.

From Eqs. (9) and (17), deviations of resonator transconductances and capacitance affect passband and stopband edges of the complex analog filter. The sensitivities of those frequencies to the resonator elements are given by

$$\left.\begin{aligned} S_{g_1}^{\omega_i} &= S_{g_3}^{\omega_i} = 1 - \frac{\omega_S}{\omega_i} \\ S_{g_2}^{\omega_i} &= \frac{\omega_S}{\omega_i} \\ S_{g_4}^{\omega_i} &= (\omega_S - \omega_i)\left(1 - \frac{\omega_S}{\omega_i}\right)\frac{x_S}{\omega_i} \\ S_C^{\omega_i} &= -1, \end{aligned}\right\} \tag{18}$$

where $\omega_i (i = 1, 2, 3, 4)$ are passband and stopband edges shown in Fig. 2. Since ω_S always exists in the passband, passband edge sensitivities become small. Thus, the proposed configuration has low sensitivity property in passband.

Deviations of g_L corresponds to that of the normalized LPF element. Sensitivity to g_L is calculated as

$$S_{g_L}^{a_i R} \quad \text{or} \quad S_{g_L}^{b_j/R} = 1. \tag{19}$$

This means that the deviation of g_L is equivallent to element deviation in the normalized LPF.

4.4 Performance Comparison between ELHT and BLLT

In the case of active realization of ELHT filters, element values of the bilinear complex resonator provided in the previous subsection are calculated from Eqs. (4) and (5) as

$$\left.\begin{aligned} g_1 &= g_3 = \sqrt{k\frac{C}{x_S}\left(2\omega_S - \frac{\omega_C}{x_S}\right)} \\ g_2 &= C\left(\omega_S - \frac{\omega_C}{x_S}\right) \\ g_4 &= \frac{k}{x_S} \\ g_L &= ka_iR \quad \text{or} \quad \frac{kb_j}{R}, \end{aligned}\right\} \tag{20}$$

where k and C are appropriate scaling coefficient, resonator capacitance, and, a_i and b_j are inductance and capacitance of the normalized LPF, respectively. Obviously, the transconductance g_1, g_2 and g_3 affect three transformation parameters of the ELHT. Any other configurations of the bilinear complex resonators [16], [17] have the same property when realizing ELHT filters. The drawback origins transformation function itself.

Therefore, active realization of ELHT filters has a disadvantage that the transformation parameters cannot be trimmed independently. Furthermore, additional hardwares which consist of division and square-root circuits are required for automatic tuning applications [7], [8].

On the other hand, in the case of BLLT filter, it is obvious from Eq. (17) that all the transconductances correspond to one specific parameter. Additional hardwares such as division and square-root circuit are not required for automatic tuning systems. It is the advantage over the ELHT in active realization.

5. A Design Example

A complex analog filter which has following specifications with Chebyshev approximation will be designed to confirm the validity of the proposed method:

$$\begin{cases} \alpha_P \le 1.0\,[\text{dB}]: & 500 \le f \le 600\,[\text{Hz}] \\ A_S \ge 30.0\,[\text{dB}]: & f \le 200, 650\,[\text{Hz}] \le f. \end{cases}$$

This is the same example that is treated in Ref. [4].

By applying the BLLT to the above specification, we have

$$\begin{cases} \omega_C = 301.593 & [\text{rad/s}] \\ \omega_S = 3518.6 & [\text{rad/s}] \\ x_S = -0.20000 & [\text{rad/s}] \\ \Omega_S = 3.0000 & [\text{rad/s}]. \end{cases}$$

From the above solution, we decide third order Chebyshev LPF as the reference. The transfer function of the destination complex filter is then given by

$$\begin{aligned} \mathbf{H}_C(s) = &-(8.0929 + j39.703) \times 10^{-4} \\ &\times \frac{s - j5026.5}{s + 147.60 - j3533.2} \\ &\times \frac{s - j5026.5}{s + 52.251 - j3764.9} \\ &\times \frac{s - j5026.5}{s + 114.05 - j3164.5}. \end{aligned}$$

Although the BLLT parameters are quite different from the ELHT, the resultant transfer function of the example is identical with ELHT design result [4]. This means that the proposed transformation, BLLT, has the design basis which minimize the order of the normalized LPF under given passband and stopband edges condition.

Figures 7 and 8 show passive complex filter structure of the example and its complex leapfrog configuration, respectively. Element values of the bilinear complex resonators are calculated as shown in Table 1.

SPICE simulations are performed by using the

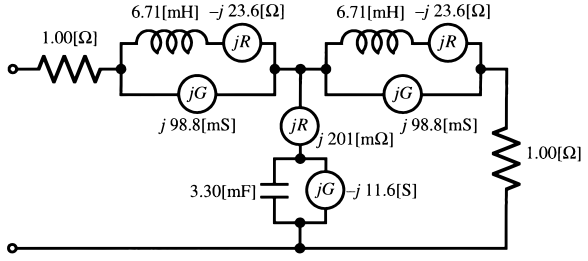

Fig. 7 A design example: passive complex filter.

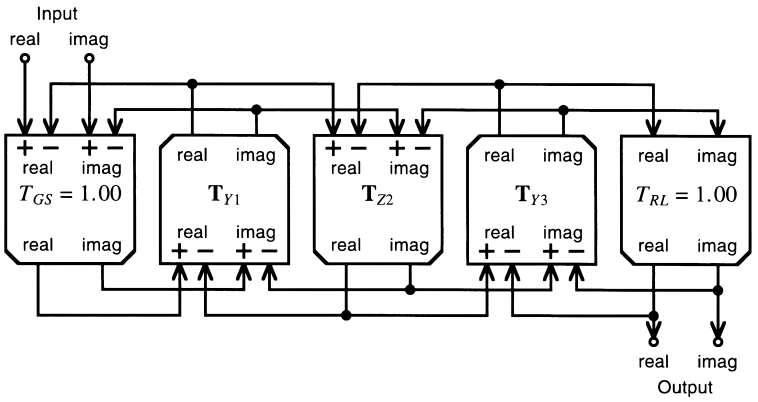

Fig. 8 The complex leapfrog configuration of the example. T_{Y1}, T_{Z2} and T_{Y3} are the bilinear complex resonator shown in Fig. 6 and Table 1. T_{GS} and T_{RL} are simulation of termination resistors.

Table 1 Element values of the OTA-C resonator.

element	series arm		shunt arm	
C	10.0	[nF]	10.0	[nF]
g_1	24.6	[μS]	24.6	[μS]
$-g_2$	35.2	[μS]	35.2	[μS]
g_3	24.6	[μS]	24.6	[μS]
g_4	40.0	[μS]	40.0	[μS]
g_L	405	[μS]	199	[μS]
g_c	0.352	[μS]	0.352	[μS]

Table 2 Sensitivities of passband and stopband edges to resonator element deviation.

x	ω_1	ω_2	ω_3	ω_4
g_1	−1.80	−0.12	0.07	0.14
g_2	2.80	1.12	0.93	0.86
g_3	−1.80	−0.12	0.07	0.14
g_4	2.70	0.03	0.01	0.05
C	1.00	1.00	1.00	1.00
Worstcase	10.10	2.39	2.08	2.19

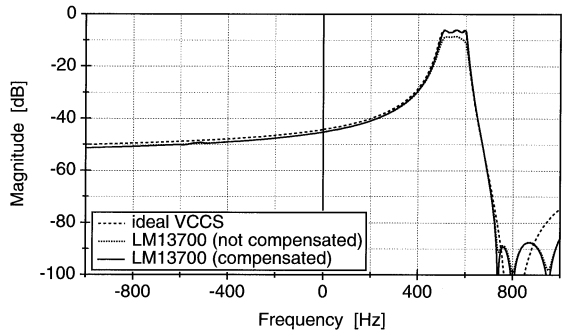

(a) Overall response.

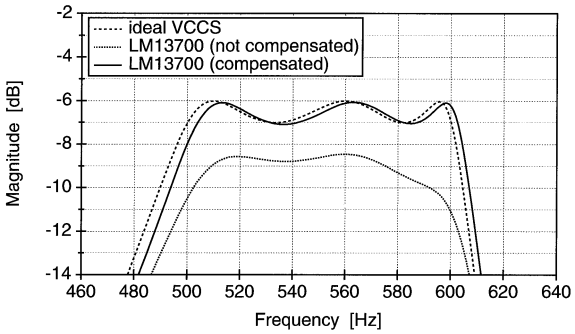

(b) Passband response.

Fig. 9 Theoretical response of the example filter.

macro model of LM13700 [18] as OTAs, which results are shown in Fig. 9. A pair of quadrature sinusoids is given as complex signal input, and real part output is evaluated. Negative value of signal frequency is obtained by inverting the polarity of the imaginary input.

Without loss compensation, passband response of the example circuit is more than 2 [dB] smaller than that of ideal one. However, compensated result agrees well with ideal one. Small amount of passband edge error can be tuned by controlling transconductance values. There also exists undesired nulls on 750 [Hz] and 950 [Hz]. These are due to phase characteristics of small valued OTAs.

Maximum input level provided by 1 [dB] output compression point is measured by the transient analysis with complex sinusoidal excitation. The result is 30 [mV] approx., which is comparable to that of a simple differential amplifier. The OTA employed in this example is just an emitter coupled BJT pair so that the dynamic range of the proposed configuration is only determined by OTA itself. Lower supply voltage, large linear input level OTAs with MOS structure [19] are recommended for actual implementation.

Passband and stopband edge sensitivities to the transconductance and capacitance deviations are calculated as shown in Table 2. Since the transformation parameter ω_S always exists in the passband, low sensitivity property of BLLT filters is verified.

6. Conclusion

In this paper, we discuss a new frequency transforma-

tion for designing complex analog filters which passband and stopband edges are arbitrary given. The bilinear LP-LP transformation (BLLT) is proposed as the special case of the extended LP-HP transformation. Parameters of the transformation and resultant filter elements are obtained by solving simultaneous equations with four unknowns. Active synthesis of BLLT filters are discussed. In a view point of controllability, it is shown that BLLT filters work better than ELHT ones. Schematic diagram of the bilinear complex resonator and its OTA-C realization which simulates branch immittances of the BLLT filter are proposed. A design example demonstrates validity of the proposed method.

If an all-pole filter is considered as the reference, the resultant complex filter has multiple zeros on the imaginary axis of the s-plane. A guideline to design complex filters with arbitrary specifications such as zero positions and independent stopband attenuations is one of the major issue of further research.

Acknowledgement

The author would thank to Dr. Noriyoshi Kambayashi of Nagaoka University of Technology, Japan, for his helpful suggestions.

References

[1] G.R. Lang and P.O. Brackett, "Complex analogue filters," Proc. European Conf. Circuit Theory Design, pp.412–419, The Hague, Netherlands, Aug. 1981.
[2] W.M. Snelgrove and A.S. Sedra, "State-space synthesis of complex analog filters," Proc. European Conf. Circuit Theory Design, pp.420–424, The Hague, Netherlands, Aug. 1981.
[3] C. Muto and N. Kambayashi, "A realization of real filters using complex resonators," IEICE Trans., vol.J75-A, no.7, pp.1181–1188, July 1992.
[4] C. Muto and N. Kambayashi, "On a design of complex transfer functions based on frequency transformation," IEICE Trans., vol.J75-A, no.11, pp.1773–1775, Nov. 1992.
[5] C. Muto and N. Kambayashi, "A leapfrog synthesis of complex analog filters," IEICE Trans. Fundamentals, vol.E76-A, no.2, pp.210–215, Feb. 1993.
[6] J. Crols and M. Steyaert, "An analog integrated polyphase filter for a high performance low-IF receiver," 1995 Symp. VLSI Circuit Digest of Tech. Papers, pp.87–88, 1995.
[7] R. Schaumann and M.A. Tan, "Continuous-time filters," in Analogue IC design: The current-mode approach, eds. C. Toumazou, F.J. Lidgey, and D.G. Haigh, pp.383–384, IEE, London, 1990.
[8] K.W. Moulding, J.R. Quartly, P.J. Rankin, R.S. Thompson, and G.A. Wilson, "Gyrator video filter IC with automatic tuning," IEEE J. Solid-State Circuits, vol.SC-15, no.6, pp.963–968, Dec. 1980.
[9] V. Belevitch, Classical Network Theory, Holden-Day, San Francisco, 1968.
[10] D.S. Humpherys, The Analysis, Design and Synthesis of Electrical Filters, Prentice-Hall, Englewood Cliffs, NJ, 1970.
[11] H.J. Orchard, "Inductorless filters," Electron. Lett., vol.2, no.6, pp.224–225, 1966.
[12] G.C. Temes and H.J. Orchard, "First-order sensitivity and worst case analysis of doubly terminated reactance two-ports," IEEE Trans. Circuit Theory, vol.CT-20, no.5, pp.567–571, Sept. 1973.
[13] H.J. Orchard, "Loss sensitivities in singly and doubly terminated filters," IEEE Trans. Circuits Syst., vol.CAS-26, no.5, pp.293–297, May 1979.
[14] C. Muto and N. Kambayashi, "Sensitivity analysis of complex lossless 2-port network," IEICE Technical Report, vol.CAS93, no.86, Nov. 1993.
[15] X. Zhang, X. Ni, M. Iwahashi, and N. Kambayashi, "Implementation of active complex filter with variable parameter using OTAs," IEICE Trans. Fundamentals, vol.E80-A, no.9, pp.1721–1724, Sept. 1997.
[16] C. Muto, "A realization of bilinear complex resonators with OTA-GC structure," IEEJ Tech. Rep., vol.ECT-98, no.85, Oct. 1999.
[17] C. Muto, "A realization of current mode bilinear complex resonators using OTAs and grounded capacitors," IEEJ Tech. Rep., vol.ECT-99, no.24, Jan. 1999.
[18] http://www.national.com/models/spice/Amplifiers/
[19] H.O. Elwan, C. Hwang, M. Ismail, and A. Hyogo, "Low voltage low power class AB OTA and V-I converter," 2nd Analog VLSI Workshop Proc., pp.57–60, Santa Clara, CA, June 1998.

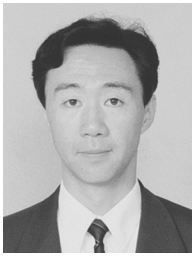

Cosy Muto was born in Hiroshima prefecture, Japan, in 1962. He received BE, ME and DE degrees in electrical engineering from Nagaoka University of Technology, Niigata, Japan in 1985, 1987 and 1994, respectively. He joined Ground Self-Defense Forces as a technology officer in 1987, where he had engaged in R&D in the field of Communications-Electronics. In 1998, he retired GSDF and have joined Takuma National College of Technology, Kagawa, Japan, where he is currently an associate professor at the Department of Telecommunications. His main research interests are the field of analog signal processing and linear circuits. Dr. Muto is a member of IEE Japan and IEEE.